Molecular Crystals and Liquid Crystals

Publication details, including instructions for authors and subscription information:
http://www.tandfonline.com/loi/gmcl20

Synthesis and Mesomorphic Properties of Symmetrical Dimers N,N′-Bis(3-Methoxy-4-Alkoxybenzylidene)-1,4-Phenylenediamine

Guan-Yeow Yeap [a], Tiang-Chuan Hng [a], Wan Ahmad Kamil Mahmood [a], Rohana Adnan [a], Masato M. Ito [b] & Yamashita Youhei [b]

[a] Liquid Crystal Research Laboratory, School of Chemical Sciences, Universiti Sains Malaysia, Penang, Malaysia

[b] Department of Environmental Engineering for Symbiosis, Faculty of Engineering, Soka University, Tokyo, Japan

Version of record first published: 31 Aug 2006

To cite this article: Guan-Yeow Yeap, Tiang-Chuan Hng, Wan Ahmad Kamil Mahmood, Rohana Adnan, Masato M. Ito & Yamashita Youhei (2006): Synthesis and Mesomorphic Properties of Symmetrical Dimers N,N′-Bis(3-Methoxy-4-Alkoxybenzylidene)-1,4-Phenylenediamine, Molecular Crystals and Liquid Crystals, 452:1, 49-61

To link to this article: http://dx.doi.org/10.1080/15421400500377743

Mol. Cryst. Liq. Cryst., Vol. 452, pp. 49–61, 2006

ISSN: 1542-1406 print/1563-5287 online
DOI: 10.1080/15421400500377743

Synthesis and Mesomorphic Properties of Symmetrical Dimers N,N′-Bis(3-Methoxy-4-Alkoxybenzylidene)-1,4-Phenylenediamine

Guan-Yeow Yeap
Tiang-Chuan Hng
Wan Ahmad Kamil Mahmood
Rohana Adnan
Liquid Crystal Research Laboratory, School of Chemical Sciences, Universiti Sains Malaysia, Penang, Malaysia

Masato M. Ito
Yamashita Youhei
Department of Environmental Engineering for Symbiosis, Faculty of Engineering, Soka University, Tokyo, Japan

A series of homologous symmetrical dimers N,N′-bis[(3-methoxy-4-alkoxybenzylidene)-1,4-phenylenediamine with different lengths of terminal alkyl groups of even parity ranging from butyl to octadecyl were prepared and characterized. Spectroscopic methods FT-IR, ^{1}H NMR, and ^{13}C NMR and mass spectrometry were carried out to determine the physical properties of the target compounds. The texture with respect to each compound within this series has been investigated along with their thermal stabilities. A diversity of phase-transition behavior was observed for the members of this series and explanation was given based on the possible molecular conformation. Almost all title compounds were nematogenic except the dimers containing butyl and hexyl chains as well as the longest octadecyl dimer in which the mesogenic properties were absent.

Keywords: N,N′-bis(3-methoxy-4-alkoxybenzylidene)-1,4-phenylenediamine; nematogenic; phase transition behaviour; symmetrical dimers; thermal stabilities

1. INTRODUCTION

The majority of the liquid crystalline compounds that have hitherto been synthesized consist of monomeric structure whereby the

Address correspondence to Guan-Yeow Yeap, currently at Department of Environmental Engineering for Symbiosis, Faculty of Engineering, Soka University, Japan. E-mail: gyyeap@soka.ac.jp or gy_yeap@yahoo.com

aromatic rings that formed the core center were connected to two flexible terminal chains such as aliphatic and alkoxy groups. Subsequent to monomeric liquid crystals, symmetrical dimers have also been isolated and characterized. The first dimer possessing liquid crystal properties was reported by Vorlander in 1927 [1]. Ever since the discovery of the mesomorphic properties of the dimeric liquid crystal, the importance features of these compounds has continually been investigated including those reported by Rault et al. in 1975 [2]. Most of the earlier reported dimers consist of a flexible central spacer connected to mesogenic segments at terminal positions [3]. In the course of the study, the scientists have also found that dimeric liquid crystals are known for exhibiting strong odd–even effects in their physical properties as the function of spacer parity [4,5].

A large number of compounds that exhibit liquid crystalline properties possess rod-like molecular shape. As a result, the molecules with *para*-positioned substituents especially those with elongated tails in the *par*a-positions of the aromatic ring will generally show liquid crystalline behavior. In contrast to this phenomenon, the thermal depression and the instability of mesophase will be observed if a substituent such as OCH_3 lies at the *ortho* and *meta* positions of the central aromatic ring system [6]. However, this interesting point does not apply to compounds with *ortho* hydroxyl groups with the azomethine (CH=N) group within its proximity in which the formation of intramolecular hydrogen bonding generally increases the stability [7].

Over past few years, a number of liquid crystalline compounds with various lateral substituents have been synthesized and extensively studied. The typical examples of compounds possess lateral hydrogen bonded phenolic group and lateral cyano group as reported by Vora and Gupta [8] and by Sakagami et al. [9], respectively. Similar to the case of molecular structure of conventional liquid crystalline compounds, molecular breadth is considered an important feature in relation to its influence on mesophase stability and clearing temperatures [10–12]. Thus, the presence of lateral substituents at the aromatic rings such as OH and OCH_3 could affect the overall mesomorphic characteristics of the liquid crystalline compounds.

Every member of the homologous series of symmetrical dimeric liquid crystalline compounds that we documented in this article contains a central aromaticring connected at both *para* positions by the azomethine group which in turn bonded to respective aromatic ring bearing the lateral OCH_3 and the elongated aliphatic chain. Both aliphatic ends are even-parity flexible alkyl chains ranging from C4 to C18, leading to the possibility of a nonpolar–polar–nonpolar sequence, which can enhance the mesomorphic behavior in comparison to the

polar-nonpolar-polar sequence described by Eidenschink [13] and Cerrada et al. [14]. The interesting aspects of the molecular structure were taken into account, which can be associated with the nematic mesophase and their relatively low clearing temperatures.

2. EXPERIMENTAL

Vanillin, *p*-phenylenediamine, potassium carbonate, 1-bromobutane, 1-bromohexane, 1-bromooctane, 1-bromodecane, 1-bromododecane, 1-bromotetradecane, 1-bromohexadecane and 1-bromooctadecane were used directly from the freshly opened bottles.

IR spectra were recorded using a Perkin Elmer 2000 FT-IR spectrophotometer in the frequency range of 4000–400 cm^{-1}. The spectra of all compounds were obtained and measured from samples in the form of KBr pellets. ^{1}H NMR and ^{13}C NMR spectra were recorded on a Bruker 400-MHz Ultrashield^{TM} FT-NMR spectrometer using $CDCl_3$ as solvent and TMS as the internal standard. CHN microanalyses were carried out using a Perkin Elmer 2400 LS Series CHNS/O analyzer. Mass spectrometry was performed on a Hewlett-Packard 5989 A mass spectrometer.

All mesophase textures observation was carried out using a Carl Zeiss Axioskop 40 polarizing optical microscope equipped with a Mettler FP52 hot stage in the Liquid Crystals Research Laboratory, School of Chemical Sciences, USM. Differential scanning calorimetry was carried out using Seiko DSC120 model 5500 in Faculty of Engineering, Soka University, at heating and cooling rates of 5°C min^{-1} and −5°C min^{-1}, respectively.

2.1. Synthesis

The syntheses of the intermediate compound **1** and its derivatives of the homologous series, **2–9** ($n = 4$–18), were carried out as summarized in Scheme 1.

2.1.1. Synthesis of Compound 1

A solution of *p*-phenylenediamine (2.163 g, 2×10^{-2} mol) in ethanol was added dropwise to a stirring 50-mL ethanolic solution of vanillin (6.542 g, 4.3×10^{-2} mol) in a round-bottom flask. The reaction mixture was then heated at 70°C for 3 h before it was left to evaporate off at room temperature. The precipitate thus isolated was then purified twice with ethanol to yield the desired intermediate compound **1**. Yield 60%. Elemental analysis: found C 70.42, H 5.49, N 7.41; calculated ($C_{22}H_{20}N_2O_4$) C 70.20, H 5.36, N 7.44. IR (KBr), 3373 cm^{-1} (OH), 1620 cm^{-1}(C=N).

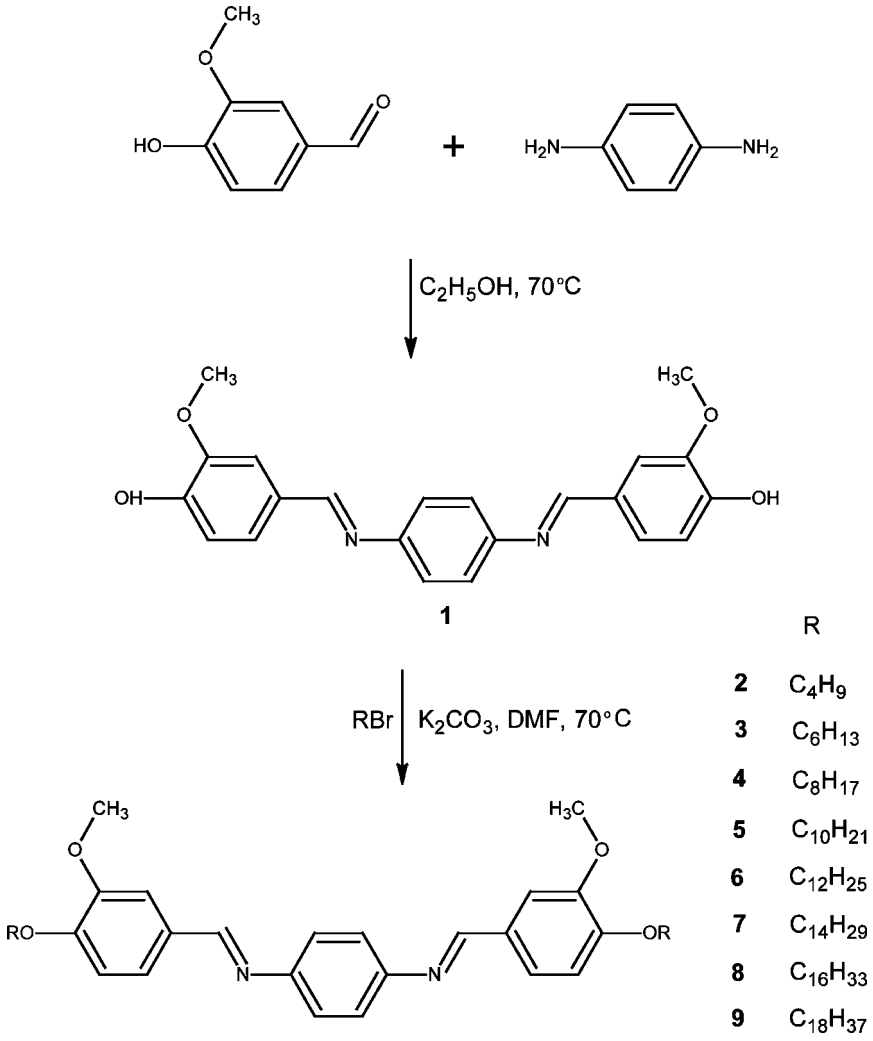

SCHEME 1

2.1.2. Synthesis of Compound 2

In a round-bottom flask, **1** (0.640 g, 1.7×10^{-3} mol) was dissolved in a N,N′-dimethylformamide solution containing K_2CO_3 (1.175 g, 8.5×10^{-3} mol). The stirring solution was heated to 40°C. 1-Bromobutane (0.507 g, 3.7×10^{-3} mol) was then added dropwise, and the mixture thus obtained was heated at 70°C for 7 h before being cooled down to room temperature. The resulting solution was then poured

into 70 mL of water, and the precipitate thus formed was filtered off and dried. The precipitate was purified with N,N′ -dimethylformamide and recrystallized with ethyl acetate to yield the desired product. Yield 73%. Elemental analysis: found C 74.63, H 7.60, N 5.69; calculated ($C_{30}H_{36}N_2O_4$) C 73.74, H 7.43, N 5.73. MS m/z: 488 (M^+). IR (KBr), 2959–2872 cm^{-1} (C−H alkyl), 1616 cm^{-1} (C=N), 1268 cm^{-1} (O−CH_2). ^{1}H NMR δ ($CDCl_3$), 0.99–1.04 ppm (t, 6H, CH_3), 1.50–1.94 ppm (m, 8H, CH_2), 3.99 ppm (s, 6H, O−CH_3), 4.11 ppm (t, 4H, O−CH_2), 6.96 ppm (d, 2H, Ar), 7.29 ppm (m, 6H, Ar), 7.63 ppm (s, 2H, Ar), 8.43 ppm (s, 2H, CH=N). ^{13}C NMR δ ($CDCl_3$), 14.26 ppm (CH_3), 19.60–31.50 ppm (CH_2), 56.49–69.14 ppm (O−CH_2), 109.73–129.82 ppm (Ar−C), 150.20–152.09 ppm (Ar−C−O), 159.60 ppm (C=N).

2.1.3. Synthesis of Compound 3

Yield 72%. Elemental analysis: found C 75.04, H 8.29, N 5.11; calculated ($C_{34}H_{44}N_2O_4$), C 74.97, H 8.14, N 5.14. MS m/z: 544 (M^+). IR (KBr), 2958–2858 cm^{-1} (C−H alkyl), 1617 cm^{-1} (C=N), 1267 cm^{-1} (O−CH_2). ^{1}H NMR δ ($CDCl_3$), 0.91–0.95 ppm (t, 6H, CH_3), 1.36–1.95 ppm (m, 16H, CH_2), 3.99 ppm (s, 6H, O−CH_3), 4.10 ppm (t, 4H, O−CH_2), 6.96 ppm (d, 2H, Ar), 7.30 ppm (m, 6H, Ar), 7.63 ppm (s, 2H, Ar), 8.43 ppm (s, 2H, CH=N). ^{13}C NMR δ ($CDCl_3$), 14.42 ppm (CH_3), 22.98–31.98 ppm (CH_2), 56.48–69.46 ppm (O−CH_2), 109.72–129.82 ppm (Ar−C), 150.19–152.08 ppm (Ar−C−O), 159.60 ppm (C=N).

2.1.4. Synthesis of Compound 4

Yield 75%. Elemental analysis: found C 75.87, H 8.89, N 4.60; calculated ($C_{38}H_{52}N_2O_4$) C 75.96, H 8.72, N 4.66. MS m/z: 600 (M^+). IR (KBr), 2957–2854 cm^{-1} (C−H alkyl), 1618 cm^{-1} (C=N), 1267 cm^{-1} (O−CH_2). ^{1}H NMR δ ($CDCl_3$), 0.88–0.91 ppm (t, 6H, CH_3), 1.31–1.95 ppm (m, 24H, CH_2), 3.99 ppm (s, 6H, O−CH_3), 4.10 ppm (t, 4H, O−CH_2), 6.96 ppm (d, 2H, Ar), 7.29 ppm (m, 6H, Ar), 7.63 ppm (s, 2H, Ar), 8.43 ppm (s, 2H, CH=N). ^{13}C NMR δ ($CDCl_3$), 14.49 ppm (CH_3), 23.05–32.20 ppm (CH_2), 56.47–69.46 ppm (O−CH_2), 109.71–129.83 ppm (Ar−C), 150.19–152.08 ppm (Ar−C−O), 159.59 ppm (C=N).

2.1.5. Synthesis of Compound 5

Yield 65%. Elemental analysis: found C 77.02, H 9.43, N 4.24; calculated ($C_{42}H_{60}N_2O_4$) C 76.79, H 9.21, N 4.26. MS m/z: 657 (M^+). IR (KBr), 2956–2853 cm^{-1} (C−H alkyl), 1618 cm^{-1} (C=N), 1266 cm^{-1} (O−CH_2). ^{1}H NMR δ ($CDCl_3$), 0.88–0.92 ppm (t, 6H, CH_3), 1.29–1.93 ppm (m, 32H, CH_2), 3.99 ppm (s, 6H, O−CH_3), 4.10 ppm (t, 4H, O−CH_2), 6.96 ppm (d, 2H, Ar), 7.30 ppm (m, 6H, Ar), 7.63 ppm (s, 2H, Ar), 8.43 ppm (s, 2H, CH=N). ^{13}C NMR δ ($CDCl_3$), 14.51 ppm

(CH_3), 23.07–32.29 ppm (CH_2), 56.47–69.46 ppm (O−CH_2), 109.71–129.82 ppm (Ar−C), 150.19–152.08 ppm (Ar−C−O), 159.60 ppm (C=N).

2.1.6. Synthesis of Compound 6

Yield 67%. Elemental analysis: found C 77.72, H 9.73, N 3.91; calculated ($C_{46}H_{68}N_2O_4$) C 77.48, H 9.61, N 3.93. MS m/z: 713 (M^+). IR (KBr), 2921–2852 cm^{-1} (C−H alkyl), 1618 cm^{-1} (C=N), 1267 cm^{-1} (O−CH_2). ^{1}H NMR δ ($CDCl_3$), 0.88–0.92 ppm (t, 6H, CH_3), 1.28–1.93 ppm (m, 40H, CH_2), 4.00 ppm (s, 6H, O−CH_3), 4.10 ppm (t, 4H, O−CH_2), 6.96 ppm (d, 2H, Ar), 7.30 ppm (m, 6H, Ar), 7.64 ppm (s, 2H, Ar), 8.43 ppm (s, 2H, CH=N). ^{13}C NMR δ ($CDCl_3$), 14.51 ppm (CH_3), 23.09–32.32 ppm (CH_2), 56.48–69.46 ppm (O−CH_2), 109.71–129.82 ppm (Ar−C), 150.19–152.08 ppm (Ar−C−O), 159.60 ppm (C=N).

2.1.7. Synthesis of Compound 7

Yield 63%. Elemental analysis: found C 78.31, H 10.07, N 3.60; calculated ($C_{50}H_{76}N_2O_4$), C 78.08, H 9.96, N 3.64. MS m/z: 770 (M^+). IR (KBr), 2920–2851 cm^{-1} (C−H alkyl), 1618 cm^{-1} (C=N),1268 cm^{-1} (O−CH_2). ^{1}H NMR δ ($CDCl_3$), 0.88–0.92 ppm (t, 6H, CH_3), 1.28–1.93 ppm (m, 48H, CH_2), 3.99 ppm (s, 6H, O−CH_3), 4.10 ppm (t, 4H, O−CH_2), 6.96 ppm (d, 2H, Ar), 7.30 ppm (m, 6H, Ar), 7.63 ppm (s, 2H, Ar), 8.43 ppm (s, 2H, CH=N). ^{13}C NMR δ ($CDCl_3$), 14.51 ppm (CH_3), 23.08–32.32 ppm (CH_2), 56.47–69.46 ppm (O−CH_2), 109.70–129.82 ppm (Ar−C), 150.18–152.07 ppm (Ar−C−O), 159.60 ppm (C=N).

2.1.8. Synthesis of Compound 8

Yield 60%. Elemental analysis: found C 78.63, H 10.38, N 3.35; calculated ($C_{54}H_{84}N_2O_4$) C 78.59, H 10.26, N 3.39. MS m/z: 825 (M^+). IR (KBr), 2919–2851 cm^{-1} (C−H alkyl), 1618 cm^{-1} (C=N), 1268 cm^{-1} (O−CH_2). ^{1}H NMR δ ($CDCl_3$), 0.90–0.92 ppm (t, 6H, CH_3), 1.28–1.90 ppm (m, 56H, CH_2), 3.99 ppm (s, 6H, O−CH_3), 4.10 ppm (t, 4H, O−CH_2), 6.96 ppm (d, 2H, Ar), 7.32 ppm (m, 6H, Ar), 7.63 ppm (s, 2H, Ar), 8.43 ppm (s, 2H, CH=N). ^{13}C NMR δ ($CDCl_3$), 14.48 ppm (CH_3), 23.07–32.31 ppm (CH_2), 56.49–69.50 ppm (O−CH_2), 109.84–129.87 ppm (Ar−C), 150.24–152.11 ppm (Ar−C−O), 159.55 ppm (C=N).

2.1.9. Synthesis of Compound 9

Yield 63%. Elemental analysis: found C 79.20, H 10.78, N 3.15; calculated ($C_{58}H_{92}N_2O_4$) C 79.04, H 10.52, N 3.18. MS m/z: 881 (M^+). IR (KBr), 2918–2850 cm^{-1} (C−H alkyl), 1618 cm^{-1} (C=N), 1268 cm^{-1} (O−CH_2). ^{1}H NMR δ ($CDCl_3$), 0.88–0.92 ppm (t, 6H, CH_3), 1.28–1.93 ppm (m, 64H, CH_2), 4.00 ppm (s, 6H, O−CH_3), 4.10 ppm (t, 4H, O−CH_2), 6.96 ppm (d, 2H, Ar), 7.30 ppm (m, 6H, Ar), 7.63 ppm (s, 2H,

Ar), 8.43 ppm (s, 2H, CH=N). ^{13}C NMR δ ($CDCl_3$), 14.52 ppm (CH_3), 23.09–32.32 ppm (CH_2), 56.48–69.47 ppm (O−CH_2), 109.70–129.82 ppm (Ar−C), 150.19–152.08 ppm (Ar−C−O), and 159.60 ppm (C=N).

3. RESULTS AND DISCUSSION

3.1. Thermal Behavior and Texture Observation

The phase-transition temperatures of the target compounds **2**–**9** are collated in Table 1. This table that only one transition temperature was observed for compounds **2** and **3** during heating and cooling processes. The enthalpies with respect to each transition in **2** (63.5 and 63.6 kJ/mol for heating and cooling cycles, respectively) and **3** (67.6 and 65.7 kJ/mol for respective heating and cooling processes) can be associated with the transition from crystal to isotropic liquid and vice versa. The high transition temperatures observed for compounds **2** and **3** could be due to the presence of a strong intermolecular attraction among the short-chain molecules leading to restricted thermal motion. As such, the molecules in compounds **2** and **3** are highly positioned, which caused the anisotropic properties of the molecules to be reduced to a remarkable extent [6]. When the length of the end tail increased to C8 as in compound **4**, two transitions were observed during the cooling cycle: first at 124.2°C (isotropic to mesophase) and followed by the transition from mesophase to crystal phase at 104.5°C. The texture observation carried out on compound **4** shows that it exists as a nematogen (Fig. 1), of which the formation of colorful marble nematic texture was observed at 114.0°C during the cooling process.

TABLE 1 Transition Temperatures and Relevant Enthalpies (kJ/mol) of Compounds **2**–**9**

Dimers	Cr → N	N → I	I → N	N → Cr
2	•	165.6 (63.5)	•	149.7 (63.6)
3	•	155.8 (67.6)	•	133.0 (65.7)
4	•	132.7 (72.5)	124.2 (49.2)	104.5 (24.7)
5	113.7 (35.7)	128.0 (53.1)	116.4 (49.5)	102.1 (39.7)
6	115.2 (48.9)	125.3 (54.3)	121.0 (52.6)	95.9 (53.3)
7	117.4 (58.7)	122.6 (52.4)	115.3 (53.1)	93.0 (61.0)
8	•	121.8 (127.8)	112.8 (53.6)	106.8 (76.7)
9	•	118.7 (139.0)	•	113.8 (55.2)

Notes: Cr, crystal; N, nematic; I, isotropic.
() represents enthalpy (ΔH_m) of the phase transition (kJ/mol).

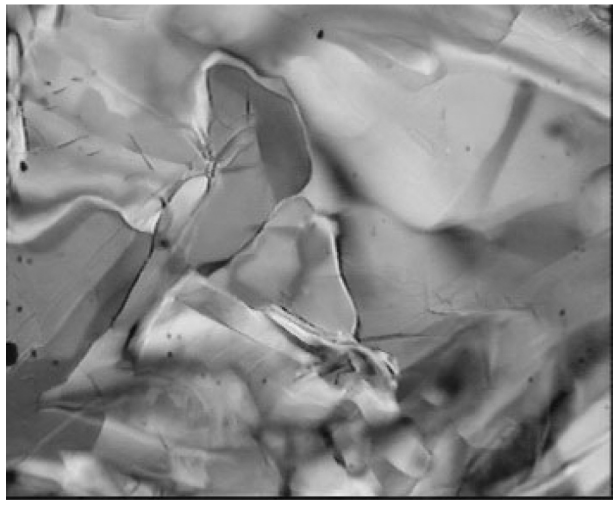

FIGURE 1 Photomicrograph of marble texture of compound **4** at 114.0°C.

A further lengthening of the end tail as we move from compound **4** to compounds **5**, **6**, and **7** has exhibited the enantiotropic behavior, the two peaks were observed in their thermograms during heating as well as cooling cycles. A representative DSC trace of compound **5** is depicted in Fig. 2. Although the Cr−N and N−I phase transitions were observed at respective temperature of 113.7°C and 128.0°C when they were heated up, the reverse process occurred at 116.4°C (I−N) and 102.1°C (N−I). The observation on compounds **5–7** under polarized light shows that the nematic phase appears during heating and cooling cycles. A typical example with regards to the texture among compounds **5–7** is illustrated by compound **6**. The nematic droplets in the isotropic matrix were observed during the cooling process (Fig. 3). As for compound **8**, a similar feature as shown by compound **4** was observed whereby the nematic phase with fine textures was only observed during the cooling process. The presence of monotropic behavior in compound **8** could possibly be due to the reduced anisotropy that destabilizes the mesomorphic properties as reported for the distinct bent-shape molecule and also the molecule possessing lateral methoxy groups [15]. This observation indicates that the molecules with the longer alkyl chain in this series are not linear. The lowering of linearity gives rise to lower clearing temperature (T_c), which is in contrast to the dimers of linear conformation, of which the T_c were found to be greater than 200°C [16]. This phenomenon has further been substantiated by the longest flexible tail containing C18 in which

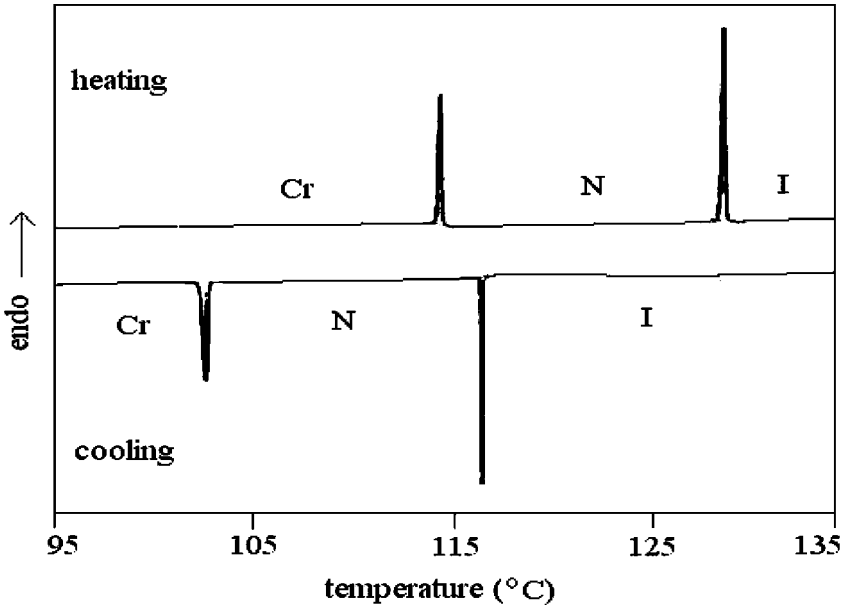

FIGURE 2 DSC trace of compound **5**.

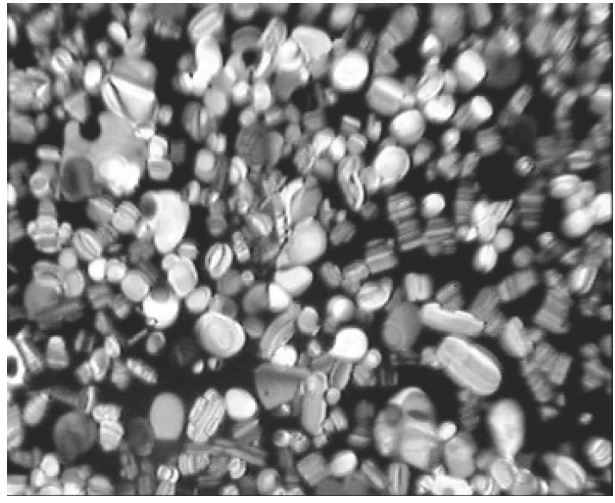

FIGURE 3 Photomicrograph of phase transition from isotropic to nematic droplets of compound **6** at 121.0°C.

the thermogram shows only one peak during heating (118.7°C) and cooling (113.8°C) processes. This observation can be associated with the direct isotropization and crystallization, suggesting that the molecule is distorted from linearity, which led to inefficient packing and lowering of the thermal stability [17].

The nematogenic behaviour observed among compounds **4**–**8** suggests that the presence of the methoxy group in the *meta* position of the aromatic system has weakened the lateral interactions between molecules, which is important for promoting higher mesophase stability, and therefore it restricts only the existence of the nematic phase [17,18]. As the series ascends from compounds **2** to **9**, it is important to note that during the heating process, the clearing points decrease gradually with increasing alkyl chain length (Fig. 4). This observation complies with previously reported homologous series of *p*,*p*′ -biphenylene esters of *p*-alkoxy and *p*-carbalkoxybenzoic acids in which the longest chain homologue has the lowest thermal stability [10]. It implies that as the alkyl chain length increases, the rigidity of the long molecular axis is further weakened and therefore the linearity of the

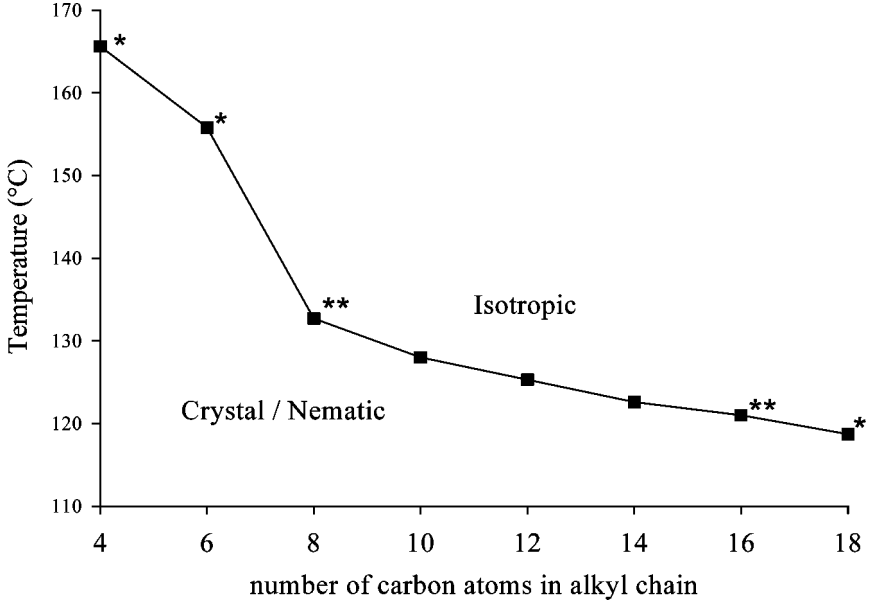

FIGURE 4 Trend of the clearing points during the heating process of compounds **2**–**9**: —■— - clearing point (during heating), ∗ - crystal to isotropic (not mesogenic), and ∗∗ - crystal to isotropic (monotropic).

molecule affected. Consequently, the molecules do not fit readily into the parallel molecular arrangement of the nematic phase due to the more significant bending conformation. As the result, the phase stability is decreased and lower transition temperatures are observed in compound **9**.

3.2. Physical Characterization

To elucidate the molecular structure of the desired compounds **2–9**, the spectroscopic techniques of FT-IR, ^{1}H NMR, and ^{13}C NMR were carried out at room temperature.

From the FT-IR spectroscopy, it was observed that the diagnostic bands assignable to the alkyl group were present within the frequencies of 2850–2919 cm^{-1} with relative intensities ranging from weakest absorption for compound **2** to the strongest for compound **9**. This characteristic is in accordance with the length of terminal alkyl groups attached to the central core in which compound **2** is the shortest member with terminal butyl groups. The bands with medium intensities were seen at 1616–1620 cm^{-1}, which can be attributed to the azomethine (CH=N) group in intermediate compound **1** as well as compound **2–9**. On the other hand, the ether group ($Ar-O-CH_2$) absorbed strongly in the frequency range of 1266–1268 cm^{-1}.

The effort to further substantiate the molecular structure determination was supported by the employment of high resolution ^{1}H and ^{13}C NMR spectroscopic techniques. From the NMR spectra, all compounds exhibited almost similar trends in terms of splitting and chemical shifts. Hence, the shortest member of the series of compound **2** was chosen for the following discussion.

From the ^{1}H NMR data of compound **2**, a triplet at $\delta = 0.99$–1.04 ppm was assigned to the methyl protons of the alkyl chain. The subsequent two sets of methylene protons at each terminal gave rise to two separate sets of multiplets within chemical shift range of $\delta = 1.50$–1.94 ppm. For the longer homologues (**3–9**), the presence of indistinguishable overlapping multiplets was observed for the methylene protons. At $\delta = 3.99$ ppm, a singlet was observed, and this can be assigned to the methoxy protons at the lateral position of the outer aromatic rings. On the other hand, the absorption of another two sets of methoxy protons which are also the methylene protons of the alkyl groups, was detected as a triplet at $\delta = 4.11$ ppm. The following set of doublet, multiplet, and a singlet within the range of $\delta = 6.96$–7.63 ppm were assigned to the four different types of aromatic protons. At low field, a characteristic singlet was observed at $\delta = 8.43$ ppm, which can be ascribed to the two azomethine protons, in which the

deshielding effect was caused by the inductive effective of N atom which reduced the electron density on adjacent C atom.

From the ^{13}C NMR data of compound **2**, the peak attributable to the methyl carbons was observed at $\delta = 14.26$ ppm. The following two peaks at $\delta = 19.60$–31.50 ppm were assigned to the two different types of methylene carbons of the alkyl groups. The methoxy carbons absorbed at $\delta = 56.49$–69.14 ppm. The aromatic proton and quarternary carbons gave rise to different peaks at $\delta = 109.73$–152.09 ppm. The appearance of another peak at $\delta = 159.60$ ppm was subsequently assigned to the azomethine carbon.

4. CONCLUSION

A series of eight novel homologous symmetrical dimers N,N′ -bis[(3-methoxy-4-alkoxy phenyl)methylene]benzene-1,4-diamine (**2**–**9**) with different terminal alkyl groups of even parity ranging from C4 (C_4H_9) to C18 ($C_{18}H_{37}$) were synthesized and characterized. All compounds were mesogenic, exhibiting nematic phase, except compounds **2**, **3**, and **9**. Although compounds **5**–**7** are enantiotropic, compounds **4** and **8** are monotropic in nature. A comparison made revealed that the nematogenic characteristics of this series can be affected by the presence of methoxy group at the *meta* position of the aromatic rings in which the mesophase and thermal stability were reduced, due to less lateral interaction among the molecules.

ACKNOWLEDGMENTS

G.-Y. Yeap thanks Universiti Sains Malaysia and the Malaysian government, especially the Ministry of Science, Technology and Innovation, for providing the facilities and Research Grant No. 305/PKIMIA/612923.

REFERENCES

[1] Vorlander, D. (1927). *Z. Phys. Chem.*, *126*, 449.
[2] Rault, J., Liebert, L., & Strzelecki, L. (1975). *Bull Soc. Chem. Fr.*, *5*, 1175.
[3] Marcelis, A. T. M., Koudijs, A., Karczmarzyk, Z., & Sudhölter, E. J. R. (2003). *Liq. Cryst.*, *30*(11), 1357.
[4] Imrie, C. T. & Luckhurst, G. R. (1998). In: *Handbook of Liquid Crystals*, Demus, D., Goodby, J., Gray, G. W., Spiess, H. W., & Vill, V. (Eds.), Weinheim: Wiley-VCH, Vol. 2B, 801.
[5] Imrie, C. T. (1999). *Struct. Bonding*, *95*, 150.
[6] Gray, G. W. (1974). In: *Liquid Crystals and Plastic Crystals*, Gray, G. W. & Winsov, P. A. (Eds.), Ellis, Horwood Ltd.: Chichester, U.K.

[7] Hirata, H., Waxman, S. N., Teucher, I., & Labes, M. M. (1973). *Mol. Cryst. Liq. Cryst.*, *20*, 343.
[8] Vora, R. A. & Gupta, R. (1979). *Mol. Cryst. Liq. Cryst. Lett.*, *56*, 31; (1980). In: *Liquid Crystals*, Chandrasekhar, S. (Ed.), Heyden Verlag, London, 589.
[9] Sakagami, S., Nonaka, K., Koga, T., & Takase, A. (1998). *Mol. Cryst. Liq. Cryst.*, *312*, 23.
[10] Dewar, M. J. S. & Schroeder, J. P. (1965). *J. Org. Chem.*, *30*, 2296.
[11] Gray, G. W., Jones, B., & Marson, F. (1956). *J. Chem. Soc.*, 1417.
[12] Berdague, P., Bayle, J. P., Ho, M. S., & Fung, B. M. (1993). *Liq. Cryst.*, *14*(3), 667.
[13] Eidenschink, R. (1979). *Kontakte (Merck)*, *1*, 15.
[14] Cerrada, P., Marcos, M., & Serrano, J. L. (1989). *Mol. Cryst. Liq. Cryst.*, *170*, 79.
[15] Rao, N. V. S., Singha, D., Das, M., & Paul, M. K. (2002). *Mol. Cryst. Liq. Cryst.*, *373*, 105.
[16] Yelamaggad, C. V., Mathews, M., Hiremath, U. S., Nair, G. G., Rao, D. S. S., & Prasad, S. K. (2003). *Liq. Cryst.*, *30*(8), 899.
[17] Perez, F., Judeinstein, P., Bayle, J. P., Roussel, F., & Fung, B. M. (1997). *Liq. Cryst.*, *22*(6), 711.
[18] Date, R. W., Imrie, C. T., Luckhurst, G. R., & Seddon, J. M. (1992). *Liq. Cryst.*, *12*(2), 203.